pp. 1–14 (2012)

Action potential propagation and phase dynamics in the sinoatrial node

R. A. SYUNYAEV*† and R. R. ALIEV*†

Abstract — We have simulated a chain of sinoatrial pacemaker cells connected *via* gap junctions. To study the dynamics we introduce a phase of oscillations and show that Burgers equation is adequate to describe the phase dynamics in the sinoatrial node. We show that the propagating action potential bears properties of either trigger waves, or phase waves, which depends upon its wave number. We propose a definition of the safety factor that is applicable to the oscillatory tissue of the sinoatrial node and show that the maximum of the safety factor relates to the boundary case separating phase waves and trigger waves.

1. Materials and methods

1.1. Mathematical model

We have simulated a chain of pacemaker cells connected *via* gap junctions to study the action potential propagation in a tissue of the sinoatrial node (SAN). Electrical dynamics of a pacemaker cell is simulated with the help of a detailed ionic model based on Hodgkin–Huxley formalism:

$$\frac{\mathrm{d}U}{\mathrm{d}t} = -\frac{1}{c_\mathrm{m}} \sum I_\mathrm{mem} \tag{1.1a}$$

$$I_\mathrm{mem} = g_i \left(\prod \alpha_{ij} \right) (U - E_i(C)) \tag{1.1b}$$

$$\frac{\mathrm{d}\alpha}{\mathrm{d}t} = \frac{\alpha_\infty(U,C) - \alpha}{\tau(U,C)} \tag{1.1c}$$

$$E = \frac{RT}{zF} \ln\left(\frac{C_0}{C_i}\right). \tag{1.1d}$$

Here, U is the transmembrane potential, c_m – membrane capacity, I_mem – transmembrane currents, g_i – maximum ion channels' conductivities; α_{ij} – gating variables, E_i – Nernst potentials, C – ion concentrations, C_o and C_i – ion concentrations outside and inside the cell, R – gas constant, T – temperature, z – ion charge, F – Faraday

*Institute of Theoretical and Experimental Biophysics, Puschino, Moscow Region, 142292 Russia

†Moscow Institute of Physics and Technology, Dolgoprudnyi, Moscow Region, 141700 Russia

The work was supported by the Russian Foundation for Basic Research (10_04_01311).

constant. The first equation (1.1a) relates the change of transmembrane potential, U to the sum of transmembrane currents; the second one describes the dynamics of ion currents close to thermodynamic equilibrium (Ohm law) (1.1b); the third one (1.1c) is the dynamics of gating variables proposed by Hodgkin and Huxley [11], in a modern interpretation the equation describes the evolution of the probability of opening and closing of ion channels; the fourth one (1.1d) – Nernst potential to describe the thermodynamic equilibrium.

This formalism is suitable to describe the dynamics of ion transfer through major membrane channels. However, some currents, e.g., the fast sodium current, I_{Na}, require a more detailed description rather then the Ohm law(1.1b). Such a description is done via solution of electro-diffusion, as is in the case of Goldman-Hodgkin-Katz flux equation [10, 12]:

$$j = P\frac{zFU}{RT}\frac{C_o - C_i e^{ZFU/RT}}{e^{zFU/RT} - 1} \tag{1.2}$$

where j is the ion flow across the membrane, P is the membrane permeability.

It should be noted that currents through ionic pumps and exchangers, i.e. I_{NaK}, $I_{\mathrm{Ca,p}}$, I_{NaCa} have to account for the change of protein conformation upon ion transfer according to the Michaelis–Menten kinetics.

The master differential equation for the transmembrane potential of an isolated pacemaker cell is as follows:

$$\begin{aligned} -C_{\mathrm{m}}\frac{\mathrm{d}U}{\mathrm{d}t} &= I_{\mathrm{Na}} + I_{\mathrm{Ca,L}} + I_{\mathrm{Ca,T}} + I_f + I_{\mathrm{Kr}} + I_{\mathrm{Ks}} + I_{\mathrm{to}} + I_{\mathrm{sus}} \\ &\quad + I_{b\mathrm{Na}} + I_{b\mathrm{Ca}} + I_{b\mathrm{K}} + I_{\mathrm{NaK}} + I_{\mathrm{NaCa}} + I_{\mathrm{Ca,p}} \end{aligned} \tag{1.3}$$

where I_{Na} – fast sodium current; $I_{\mathrm{Ca,T}}$ and $I_{\mathrm{Ca,L}}$ are Ca^{++} L and T type currents; I_f – hyperpolarization-activated current; I_{Kr} and I_{Ks} – rapid and slow delayed rectifying potassium current; I_{to}, I_{sus} – 4-AP sensitive currents; $I_{b\mathrm{Na}}$, $I_{b\mathrm{Ca}}$, $I_{b\mathrm{K}}$ – background currents; I_{NaK} – Na-K ATPase current; I_{NaCa} – Na-Ca exchanger current; $I_{\mathrm{Ca,p}}$ – Ca^{++} pump current.

In addition, we have accounted for the change of intracellular sodium, potassium and calcium ion concentrations by estimating the net sum of appropriate transmembrane ion flows: $j = I(U,C)/zF$.

The calcium ions concentration was estimated at four different cell compartments: myoplasm, calcium uptake from myoplasm to network sarcoplasmic reticulum (NSR) by the SERCA-2 pump, concentration in junctional sarcoplasmic reticulum (JSR) to which calcium ions diffuse from NSR, and Ca^{++} concentration in the dyadic subspace. The diffusion from JSR to NSR and from the dyadic subspace to myoplasm was estimated as $j_{Ca} = (C_1 - C_2)/\tau$, where C_1 and C_2 are the concentrations of Ca^{++} at the corresponding compartments. The model also accounts for calcium bufferization by tropnin-C, calmodulin, and calsequestrin.

A detailed list of a single SAN pacemaker-cell model equations and numeric constants can be found in the references [2, 4–6, 20, 21]. In addition to central and

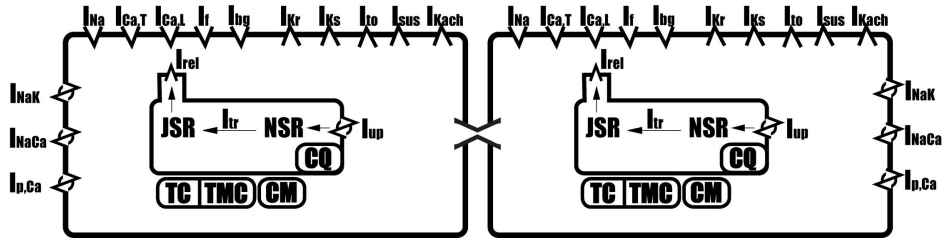

Figure 1. Scheme of two SAN pacemaker cells coupled electrically *via* gap junctions. Depicted membrane currents and sarcoplasmatic reticulum elements are listed in the text.

peripheral cells [20] we have also modelled intermediate cells linearly interpolating the parameters $p(ct) = p_c + ct(p_p - p_c)$, where ct is the cell type, varying from 0 to 1, p_c and p_p are the respective extremes (central and peripheral) of the parameter values [16].

The interaction of cardiocytes *via* gap junctions (see Fig.1) was simulated by assuming junctions to be constant-resistance conductors : $I_{gap} = g_{gap}(U_1 - U_2)$. Gap junction conductivities, g_{gap}, inside SAN were set to $4nS$, which is consistent with the experiment [19], and large enough to synchronize the cells [16].

Differential equations were integrated using the Euler method. Differential equations of simple relaxation (1.1c) were integrated directly assuming constant coefficients during a time step:

$$\alpha(t + \mathrm{d}t) = \alpha_\infty - (\alpha_\infty - \alpha)\exp(-\mathrm{d}t/\tau). \tag{1.4}$$

We used time steps of $10^{-5}s$ or less to adequately simulate the fastest sodium current. It should be noted that such small time steps are not a restriction of the simple method of integration applied, but result from the physical nature of the simulated processes. The transmembrane potential, ion concentrations, and other parameters were assumed uniform within a single cell, i.e., the spacial steps correspond to the size of a cardiocyte (70μ m [7]).

1.2. Burgers equation

To study the phase dynamics we have simulated 1D chains composed of one hundred SAN pacemaker cells of the same type coupled *via* gap junctions. We used an impermeable wall as the boundary condition. For a single pacemaker cell the phase was defined as $\varphi(t) = 2\pi(t - t_0)/(t_1 - t_0)$, where t_0 and t_1 are two successive moments of fast cell depolarization formally defined as: $U_m = -30\,\mathrm{mV}$ and $\mathrm{d}U_m/\mathrm{d}t > 0$. To estimate the wave number and Laplacian of the phase, $\bigtriangledown\varphi$ and $\bigtriangleup\varphi$, we used finite differences $k(t,x) = \bigtriangledown\varphi(t,x) = (\varphi(t,x+h) - \varphi(t,x-h))/2h$, $\bigtriangleup\varphi(t,x) = (k(t,x+h) - k(t,x-h))/2h$, h is the spatial step equal to the size of the cell.

To study the evolution of the phase in space and time we applied initial conditions in the form of a sine wave: $\varphi(0,x) = \pi(1 + \sin(k_{max}x))$, with a constant k_{max}

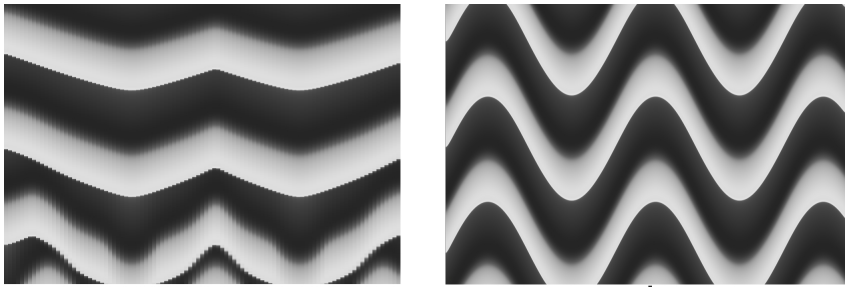

(a) (b)

Figure 2. Synchronization in a chain of oscillating SAN pacemaker cells. Evolution of phase disturbances is shown. Vertical axis stands for time from 0*s* to 0.700*s*; horizontal axis – space. White color – depolarization, black – repolarization. The panel (a) corresponds to 100 cells in the chain, (b) – 1000 cells in the chain.

that was assumed to be $2.14\,\mathrm{mm}^{-1}$ except for the Fig. 2b where it was ten times lower. In such inhomogeneous phase system, the phase shifts between the neighbour cells result in electrical currents through the gap junctions, which result in synchronization of the oscillations of coupled pacemaker cells [16] (see Fig. 2a).

Note that phase shifts occur at the boundaries of the cells where cells are connected *via* gap junctions (see Fig. 2a). If we run a system ten times longer composed of a thousand of cells (see Fig. 2b), the phase shifts between the cells become invisible. However, the latter case is physiologically unrealistic due to the limitations on the size of the SAN, thus, it is the case 'a' and not 'b' of Fig. 2.

The proposed technique has allowed us to study the dynamics in a wide range of spacial and temporal frequencies, ω (circular frequency), $\bigtriangledown\varphi$ and $\bigtriangleup\varphi$. According to Burgers equation interpretation for non-linear systems as given in [3, 13]:

$$\frac{\mathrm{d}\varphi}{\mathrm{d}t} = \omega_0 + A(\bigtriangledown\varphi)^2 + D(\bigtriangleup\varphi) \tag{1.5}$$

the verification of this relation between the above mentioned parameters was one of the purposes of this study.

1.3. Safety factor

The safety factor is a dimensionless parameter that indicates the margin of safety under which the action potential propagates relative to the minimum requirements for sustained conduction [15]. Several attempts to numerically estimate the safety factor for an excitable tissue have been done [9, 14, 15]. However, these attempts have been concentrated on excitable tissue exclusively, which is suitable for a working myocardium, and none of them is adequate for a spontaneously active tissue, i.e. the SAN tissue, as we show in the next section. We propose a new definition of the safety factor that is applicable to an oscillatory SAN tissue.

The idea of the safety factor is based upon the fact that the action potential is generated by currents through both membrane ion channels and gap junctions con-

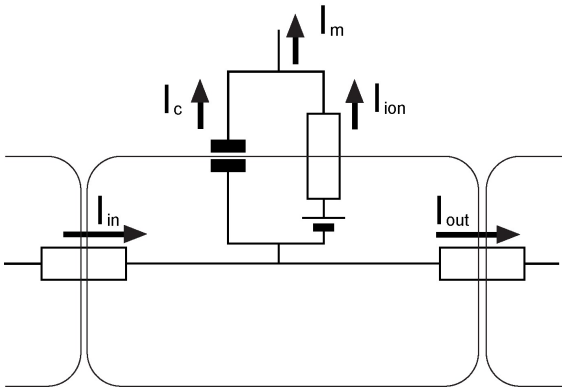

Figure 3. Currents in coupled cells: I_{m} – total transmembrane current is composed of ionic, I_{ion}, and capacitive, I_{c}, currents. I_{in} and I_{out} are axial currents to and from the cell due to gap junctions.

necting neighbour cells. To understand the electricity of a cell, consider an equivalent current network in coupled cells (see Fig. 3). Note that the net membrane current I_{m} can be written in two alternative ways: $I_{\mathrm{m}} = I_{\mathrm{c}} + I_{\mathrm{ion}} = I_{\mathrm{in}} - I_{\mathrm{out}}$. When the action potential reaches the upstream neighbouring cell, the voltage gradient between the two cells causes a current through gap junctions (I_{in} is supposed to be positive at the moment). This, in turn, results in the cell membrane depolarization (current through the capacitor, I_{c}), and a current to the downstream cell ($I_{\mathrm{out}} > 0$, when the cell under consideration charges the downstream cell). I_{ion} is the net current through the membrane channels (which is equal to the $\sum I_{\mathrm{mem}}$ in (1.1a). Outward currents I_{ion}, I_{c}, I_{m}, I_{out} are assumed to be positive. These introduced currents have allowed us to define the safety factor as:

$$SF = 1 - \frac{\int_{I_{\mathrm{m}}>0, I_{\mathrm{ion}}<0} I_{\mathrm{m}} \mathrm{d}t}{\int_{I_{\mathrm{ion}}<0} I_{\mathrm{ion}} \mathrm{d}t}. \tag{1.6}$$

We were particularly interested in the safety factor dependence on the wave number. For this purpose we simulated a chain of cells, the last cell to be coupled with the first one; thus we assumed the periodic boundary conditions. One can imagine this as a one-dimensional ring of cells. The convenience of this approach is that we could vary the wave number simply by changing the number of cells in the chain using the following phase dependence along the coordinate $\varphi(x) = 2\pi x/L$, where L is the length of chain. The wave number, in turn, affected the period of cell oscillations. The value of the safety factor was estimated in a sample cell of the ring of cells.

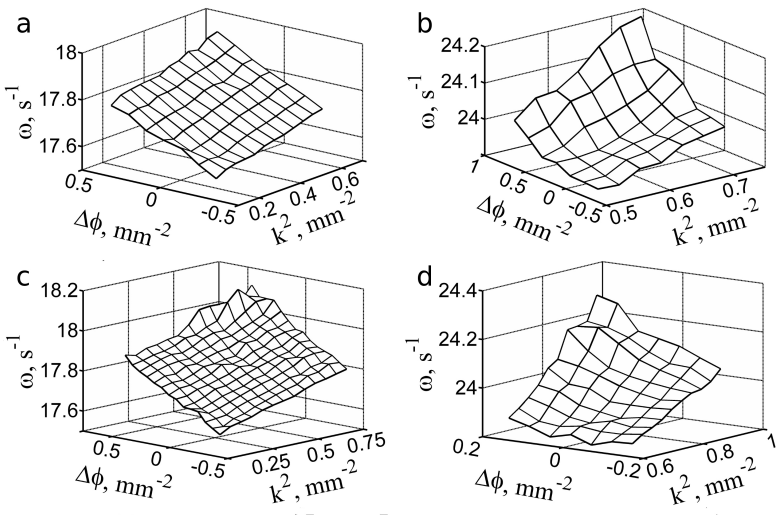

Figure 4. Relationships between temporal and spatial frequencies ω, k and $\triangle\varphi$. Burgers equation assumes a linear dependence of the parameters meaning the planes in the plot. The panel (a) – corresponds to the central cells, (b) – peripheral cells, (c) – intermediate type 0.25, (d) – intermediate type 0.5.

2. Results

The transmembrane potential in the SAN tissue composed of connected cells can be found by solving an ODE:

$$-c_{\mathrm{m}}\frac{\mathrm{d}U}{\mathrm{d}t} = \sum I_{\mathrm{mem}} + \sum I_{\mathrm{gap}} \tag{2.1}$$

where I_{mem} – currents through the membrane channels, I_{gap} – currents through gap junctions. If $\sum I_{\mathrm{gap}}$ is a small perturbation, the finite differences are naturally approximated with derivatives to give a PDE:

$$\frac{\mathrm{d}U}{\mathrm{d}t} = \bigtriangledown(D\bigtriangledown U) - \frac{1}{c_{\mathrm{m}}}\sum I_{\mathrm{mem}}. \tag{2.2}$$

This equation is known as a reaction-diffusion equation, therefore, we can apply the Burgers equation to describe the phase dynamics in the SAN tissue, provided the phase shifts between neighbouring cells are small (see Appendix A, [13]).

We have simulated the system of ODEs (2.1) as described in Section 1.2 to find relationships between the terms of Burgers equation (1.5) ω, $\bigtriangledown\varphi$ and $\triangle\varphi$. The relationships are plotted in Fig. 4. It should be noted that each node on the plot is actually an average of a few hundreds of points. It can be seen that Burgers equation assuming a simple linear dependence between ω, $\bigtriangledown\varphi$ and $\triangle\varphi$ describes the dependencies between the quantities reasonably well for different types of SAN cells.

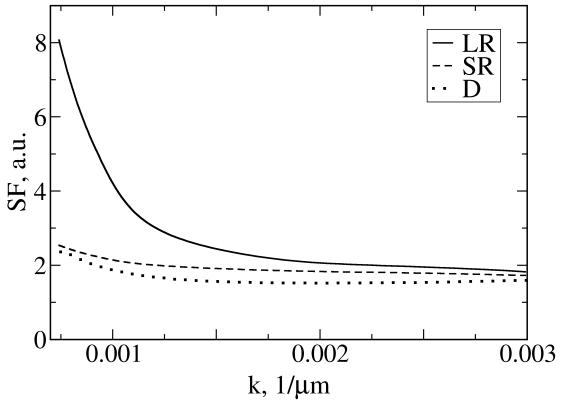

Figure 5. Ordinary safety factor estimations for central SAN pacemaker cells. Note high values of SF as wave number tends to zero.

Table 1.

cell type	A, $10^5 \mu\mathrm{m}^2/s$	D, $10^5 \mu\mathrm{m}^2/s$	ω_0, s^{-1}
0	0.91 ± 0.08	1.09 ± 0.05	17.653 ± 0.010
0.25	0.99 ± 0.04	1.12 ± 0.03	17.645 ± 0.006
0.5	3.40 ± 0.16	0.85 ± 0.11	23.22 ± 0.04
1	2.8 ± 0.8	1.1 ± 0.3	23.43 ± 0.15

The coefficients of (1.5) obtained by the weighted least squared evaluation are presented in Table 1.

Because Burgers equation in its ordinary form (1.5) is applicable only in the case of small phase gradients, it does not allow one to discriminate different regimes of propagation that occur under small and large wave numbers. The concept of the safety factor may serve this purpose. The literature suggests a few SF formulations, which we discuss later: by Delgado (D) [9], by Leon and Romberge (LR) [14], by Shaw and Rudy (SR) [15] (see Appendix B for formulae).

We have estimated these SF applied to the SAN tissue and found that LR, SR and D safety factors tend to increase as the phase shifts between cells are small (see Fig. 5), i.e. these are large, predicting 'safe' propagation, when interaction between cells is negligible, and no electrical charge, no information is carried over during propagation. Such propagation, despite the indications of SFs, is obviously unsafe, because the cells depolarize and repolarize independently of their neighbours, therefore, such propagation, for example, cannot synchronize the contraction of myocardium for the heart to work as a pump. The working safety factor indicator is supposed to decrease for such propagation. In this work we propose a safety factor (1.6) which remains small when the phase shifts between cells are small, as well as

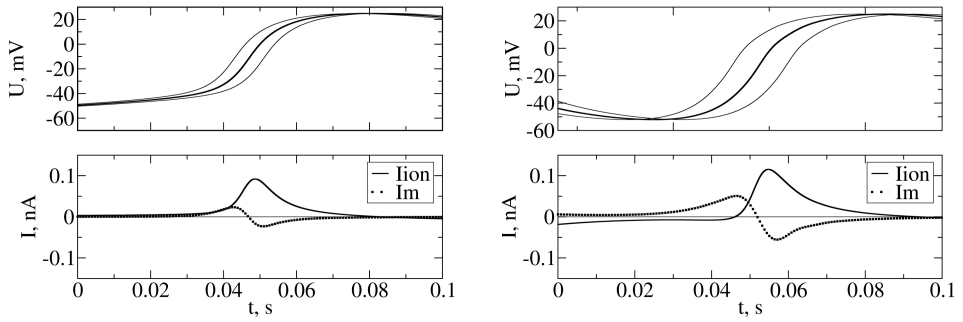

Figure 6. Dynamics during wave propagation in a ring of 125 (a) and 28 (b) cells. Upper panel: action potentials for a sample pacemaker cell (thick line) and for its adjacent neighbours (thin lines). Lower panel: currents in the sample cell *vs* time.

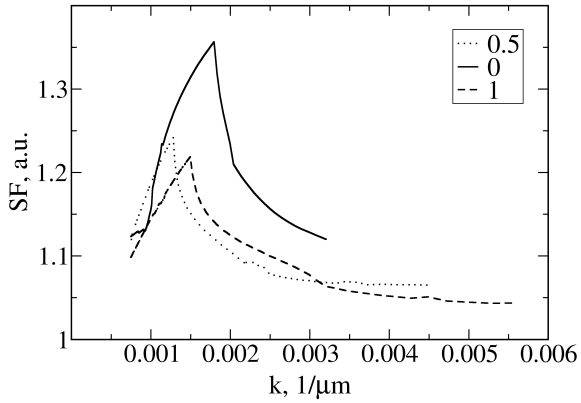

Figure 7. Safety factor estimations for central (0), peripheral (1) and intermediate (0.5) SAN pacemaker cells. X axis stands for the wave number, Y – safety factor.

in the case of large wave numbers, when the front of a wave runs into refractoriness, disturbing normal propagation.

The safety factor (1.6) meets the aforementioned requirements as can be seen in Fig. 6. Indeed, $I_{\rm m} = I_{\rm in} - I_{\rm out}$ tends to be small in the case of weakly interacting cells (Fig. 6a), which decreases the numerator of the safety factor (1.6). With the increase of the phase shifts between neighbouring cells, currents through the gap junctions increase too; so does the shift between the areas $I_{\rm ion} < 0$ and $I_{\rm m} > 0$ (see Fig. 6b). Therefore the numerator domain of integration in (1.6) is tiny in the case of large wave numbers. The introduced safety factor has been estimated for different wave numbers for central, peripheral and intermediate type cells (see Fig. 7). An additional advantage of the safety factor (1.6) is that we avoid a decomposition of the current into its inward and outward components, which is particularly troublesome in a realistic distributed syncytium of the SAN with a rather irregular grid.

3. Discussion

It is known that heart rhythms formation in the SAN is a complex non-linear process, which is difficult to analyze. In particular, the phase shifts in the oscillatory activity of pacemaker cells occurring in the SAN [16] are essential for the dynamics and result in complex changes of the membrane and inter-cellular currents, which, in turn, affects the period of oscillations, the shape of the action potential, and many other aspects of the myocardium electrical activity. One of the major goals of the current work was to develop tools and indicators to simplify analysis of complex oscillatory dynamics in a distributed network of connected nonlinear oscillators, dynamics in the SAN tissue. In particular, we have concentrated on the effects of the phase shifts and wave numbers on the propagation in the SAN and propose a few techniques, such as the Burgers equation and the safety factor, to simplify and to help understanding the dynamics.

We introduce a safety factor (1.6) that is suitable for oscillating SAN tissue. It should be noted that the safety factor is a useful concept to analyze propagation in cardiac tissue, which is a topical line of research. This is exemplified by recent studies by Boyle and Vigmond [8], who suggested a reformulation of the safety factor with an accent on spatial effects during a two-dimensional propagation through the Purkinje-ventricular junction.

It is conventional to distinguish two basic types of propagation in an oscillating medium: trigger waves and phase waves [1]. As applied to cardiac tissue, trigger waves are relatively slow (10 to 100 cm/s) waves of the action potential similar to the ones observed in a working myocardium of ventricles and atria. The second type of waves, which is exclusively due to oscillatory properties of the SAN, are phase waves, whose velocity is multiply superior to the velocity of trigger ones, with no upper limit for the velocity. These waves occur at low phase gradients and are, obviously, unable to carry information with propagation. It should be noted these are the two ultimate cases and no strict boundary between them has been observed in chemical systems [1,3]. Such is the case of the SAN tissue, as is shown here. In addition to the two above types of waves it is reasonable to introduce an intermediate type of wave, phase-diffusion waves that propagate faster than trigger waves and can carry some information because they do initiate electrical currents, and diffusion of ions between cells. These waves are located on the flat segment of the dispersion curve $v(T)$ (note that the periods T and wave numbers k in Figs. 7 and 8 are bounded as: $kvT = 2\pi$).

The dispersion curves for 1D propagation in the SAN are depicted on the lower panel of Fig. 8. Note the asymptote: phase speed $v = \lambda/T$ (λ – wave length, T – period of cells oscillations) tends to infinity, while T tends to the period of unperturbed oscillations. In the vicinity of this asymptote the wave numbers are small, the interactions between the cells are weak and the propagation is seen in the form of phase waves. Consequently (the interaction between cells is a small perturbation) the dynamics of such waves may be described by the Burgers equation. However, one can see that while there is an almost perfect linear dependence between ω, k and

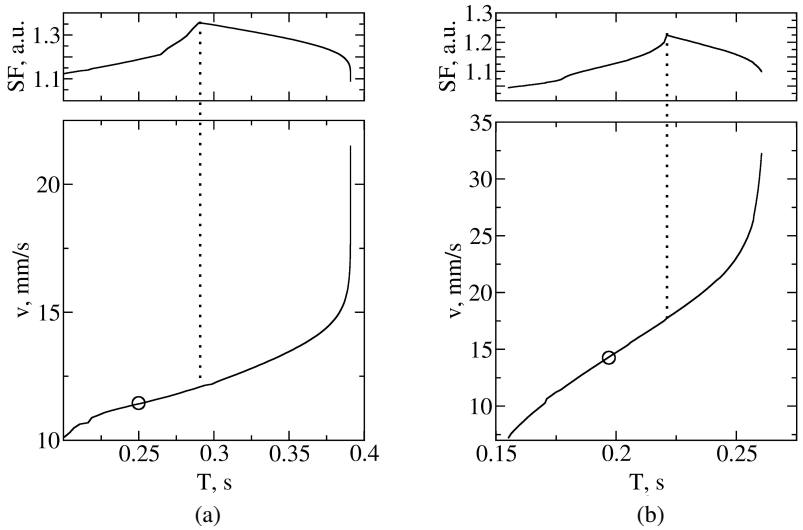

Figure 8. Safety factor *vs* dispersion relation for central (a) and peripheral (b) cells. The circle marks the point of inflection of the dispersion curve to be a border indicator between the phase and trigger waves [3].

$\triangle\varphi$ for the central cells and intermediate type cells 0.25 (see Figs. 4a and 4c), the dependencies for peripheral cells and intermediate cells 0.5 are not that plane (see Figs. 4b and 4d). This may be correlated with the fast sodium currents occurring in these cells that are absent in central cells. Additional terms are likely to be included in the equation to describe the peripheral cells.

On the left part of the dispersion curve, the wave numbers are large; the slow spontaneous depolarization phase is driven not by the membrane currents, but by the interaction between the neighbouring cells (see Fig.6b). This dynamics is similar to the excitable tissue of a working myocardium, consequently, we can classify these waves as trigger waves.

The point of inflection on the dispersion curve may be used as a formal boundary between these two propagation modes [3]. The safety factor defined in the current work is actually based on the phase shifts between the domains $I_{\rm ion} < 0$ and $I_{\rm m} = I_{\rm in} - I_{\rm out} > 0$ (1.6) and, therefore, may also serve the same purpose. However, the two do not coincide (see Fig. 8), indicating that there is no strict boundary between the phase and trigger waves. An obvious geometrical explanation for the fact is that the point of inflection lies in a broad region with the small second derivative $\mathrm{d}^2v/\mathrm{d}T^2$. This form of the dispersion relation $v(T)$ is not unique for the SAN tissue studied here, but has been observed in chemical systems as well [3]. Such a form of the dispersion curve seems to be universal and, firstly, explains why there is no coincidence of the two formal margin points between the phase and trigger waves (the inflection point and the safety factor); secondly, it justifies the phase-diffusion waves introduced above as a new class of waves in a nonlinear oscillatory system.

Here we study the dynamics in a one-dimensional system. This simplified

approach has allowed us to observe novel interesting relationships between *phase-diffusion* waves, Burgers equation and the safety factor. A further detailed research of the phenomena in more realistic 2D and 3D geometries, as we have done for analysis of pattern formation in the SAN [17, 18], is badly needed.

Appendix A

Burgers equation applied to phase dynamics in oscillating media has been introduced by Kuromoto [13]. Here we sketch the physical essence of this idea. If X_0 is a stable T-periodical solution of an n-dimensional system of ODE, or

$$\frac{\mathrm{d}X_0}{\mathrm{d}t} = F(X_0),\ X_0(t+T) = X_0(t) \tag{A.1}$$

and the vector field is perturbed as

$$\frac{\mathrm{d}X}{\mathrm{d}t} = F(X) + \varepsilon p(x) \tag{A.2}$$

and C denotes a closed orbit corresponding to $X_0(t)$, then we can define the phase φ as

$$\frac{\mathrm{d}\varphi(X)}{\mathrm{d}t} = 1, \quad X \in C. \tag{A.3}$$

If we define the asymptotic phase in some vicinity of C (see [13] for details), then

$$\frac{\mathrm{d}\varphi(X)}{\mathrm{d}t} = \mathrm{grad}_X \varphi\ \frac{\mathrm{d}X}{\mathrm{d}t} = \mathrm{grad}_X \varphi[F(X) + \varepsilon p(X)] = 1 + \varepsilon p(X)\mathrm{grad}_X \varphi. \tag{A.4}$$

This equation is exact, but below we will consider X to be in a close vicinity of C to get rid of the X dependence in $p(X)$ and $\mathrm{grad}_X \varphi$. If a small perturbation is a diffusion operator $\varepsilon p(X) = D\bigtriangledown^2$, i.e. (A.2) is a reaction-diffusion equation, then one can show (see [13] for details) that

$$\frac{\partial \varphi}{\partial t} = 1 + \Omega^{(1)}(\varphi) \bigtriangledown^2 \varphi + \Omega^{(2)}(\varphi)(\bigtriangledown \varphi)^2 \tag{A.5a}$$

$$\Omega^{(1)}(\varphi) = Z(\varphi) D \frac{\mathrm{d}X_0(\varphi)}{\mathrm{d}\varphi} \tag{A.5b}$$

$$\Omega^{(2)}(\varphi) = Z(\varphi) D \frac{\mathrm{d}^2 X_0(\varphi)}{\mathrm{d}\varphi^2} \tag{A.5c}$$

$$Z(\varphi) = (\mathrm{grad}_X \varphi)_{X = X_0(\varphi)}. \tag{A.5d}$$

In order to achieve the mean frequency:

$$\frac{\partial \varphi}{\partial t} = 1 + \alpha \bigtriangledown^2 \varphi + \beta (\bigtriangledown \varphi)^2 \tag{A.6a}$$

$$\alpha = \frac{1}{T} \int_0^T \Omega^{(1)}(t) \mathrm{d}t \tag{A.6b}$$

$$\beta = \frac{1}{T} \int_0^T \Omega^{(1)}(t) \mathrm{d}t. \tag{A.6c}$$

This is Burgers equation for reaction–diffusion systems.

Appendix B

There are few definitions of the safety factor known in the literature. Delgado's definition [9] is based upon an intuitive understanding of the safety factor, D, as a fraction of the incoming charge bringing the cell to the threshold: the ratio of the total charge generated by the inward current to the charge generated by the inward current before the membrane potential reaches the threshold.

$$SF_D = \frac{\int_{I_{\mathrm{in}}>0} I_{\mathrm{in}} \mathrm{d}t}{\int_{I_{\mathrm{in}}>0, t<\mathrm{treshold}} I_{\mathrm{in}} \mathrm{d}t}. \tag{B.1}$$

We used $-50\,\mathrm{mV}$ as the threshold potential; strictly speaking, there is no threshold potential value for the SAN cells. When the phase shifts between the cells are small, the numerator is much larger then the denominator, because of the larger potential gradient during the rapid depolarization phase. Greater wave numbers cause both the numerator and the denominator growth, but the denominator grows faster (see Fig. 5).

Leon and Romberge [14] have proposed the safety factor, LR, as a ratio of the charge generated by inward ionic currents I_{ion} to the charge generated by the total inward membrane current I_{m} (see Fig. 3):

$$SF_{LR} = \frac{\int_{I_{\mathrm{ion}}<0} I_{\mathrm{ion}} \mathrm{d}t}{\int_{I_{\mathrm{m}}<0} I_{\mathrm{m}} \mathrm{d}t}. \tag{B.2}$$

This safety factor tends to infinity when the wave number tends to zero, because $I_{\mathrm{ion}} = -I_{\mathrm{c}}$ in the case of non-interacting cells.

Shaw and Rudy [15] have developed a definition of the safety factor SR based upon the ratio of the total charge 'produced' by the cell to the total

charge 'consumed' [15]:

$$SF_{SR} = \frac{\int_{Q_m>0} (I_c + I_{out})\mathrm{d}t}{\int_{Q_m>0} I_{in}\mathrm{d}t}\,. \tag{B.3}$$

The integrals are evaluated from the start of the membrane depolarization to the point when Q_m returns to zero. Here, in the case of the oscillatory tissue, I_{in} and I_{out} tend to zero, as the wave number tends to zero, however these variations of the wave number have almost no effect on I_c, consequently, the SR safety factor also tends to infinity.

References

1. R. R. Aliev. Oscillation phase dynamics in the belousov-zhabotinsky reaction. implementation to image processing. *J. Phys. Chem.* (1994) **98**, No. 15, 3999–4002.
2. R. R. Aliev. *Conceptual and Detailed Models of Electrical Activity of the Myocardium*. Lambert Academic Publishing, 2012 (in Russian).
3. R. R. Aliev and V. N. Biktashev. Dynamics of the oscillation phase distribution in the bz reaction. *J. Phys. Chem.* (1994) **98**, No. 38, 9676–9681.
4. R. R. Aliev and L. M. Chailakhyan. Study of the effect of acetylcholine on intracellular homeostasis of true pacemaker cells of rabbit sinus node using computer simulation. *Doklady Biochem. Biophys.* (2005) **402**, No. 1, 236–239.
5. R. R. Aliev, V. V. Fedorov, and L. V. Rosenshtrakh. Simulation of ACh effects on ionic current of primary and subsidiary pacemakers single cells of rabbit sinoatrial node. *Doklady Biolog. Sci.* (2004) **397**, No. 5, 697–700.
6. R. R. Aliev, V. V. Fedorov, and L. V. Rosenshtrakh. Study of the effect of acetylcholine on the excitability of true pacemaker cells of rabbit sinus node using computer simulation. *Doklady Biolog. Sci.* (2005) **402**, No. 4, 548–550.
7. M. R. Boyett, H. Honjo, I. Kodama, M. K. Lancaster, M. Lei, H. Musa, and H. Zhang. The sinoatrial node: cell size does matter. *Circ. Res.* (2007) **101**, No. 7, e81–e82.
8. P. M. Boyle and E. J. Vigmond. An intuitive safety factor for cardiac propagation. *Biophys.* (2010) **98**, No. 12, L57–L59.
9. C. Delgado, B. Steinhaus, M. Delmar, D. R. Chialvo, and J. Jalife. Directional differences in excitability and margin of safety for propagation in sheep ventricular epicardial muscle. *Circ. Res.* (1990) **67**, No. 1, 97–110.
10. D. E. Goldman. Potential, impedance, and rectification in membranes. *J. Physiol.* (1943) **27**, No. 1, 37–60.
11. A. L. Hodgkin and A. F. Huxley. A quantitative description of membrane current and its application to conduction and excitation in nerve. *J. Physiol.* (1952) **117**, No. 4, 500–544.
12. A. L. Hodgkin and B. Katz. The effect of sodium ions on the electrical activity of the giant axon of the squid. *J. Physiol.* (1943) **108**, No. 1, 37–77.
13. Y. Kuramoto. *Chemical Oscillations, Waves, and Turbulence*. Springer-Verlag, Berlin–Heidelberg–New York–Tokyo, 1984.

14. L. J. Leon and F. A. Roberge. Directional characteristics of action potential propagation in cardiac muscle. a model study. *Circ. Res.* (1991) **69**, No. 2, 378–395.

15. R. M. Shaw and Y. Rudy. Ionic mechanisms of propagation in cardiac tissue. roles of the sodium and l-type calcium currents during reduced excitability and decreased gap junction coupling. *Circ. Res.* (1997) **81**, No. 5, 727–741.

16. R. A. Syunyaev and R. R. Aliev. Modelling of the influence of gap-junction coupling on synchronization of central and peripheral sinoatrial node cells. *Biophys.* (2009) **54**, No. 1, 58–60.

17. R. A. Syunyaev and R. R. Aliev. Computer simulations of pacemaker shift in the sinoatrial node. *Biophys.* (2010) **55**, No. 6, 1025–1029.

18. R. A. Syunyaev and R. R. Aliev. Computer simulation of 3D electrical activity in the sinoatrial node. *Russ. J. Numer. Anal. Math. Modelling* (2011) **26**, No. 6, 575–587.

19. S. Verheule, M. J. Van Kempen, S. Postma, M. B. Rook, and H. J. Jongsma. Gap junctions in the rabbit sinoatrial node. *Amer. J. Physiol.* (2001) **280**, No. 5, H2103–H2115.

20. H. Zhang, A. V. Holden, I. Kodama, H. Honjo, M. Lei, T. Varghese, and M. R. Boyett. Mathematical models of action potentials in the periphery and center of the rabbit sinoatrial node. *Amer. J. Physiol.* (2000) **279**, No. 1, H397–H421.

21. H. Zhang, A. V. Holden, D. Noble, and M. R. Boyett. Analysis of the chronotropic effect of acetylcholine on sinoatrial node cells. *J. Cardiovasc. Electrophysiol.* (2002) **13**, No. 5, 465–474.